



Published in final edited form as:

*Mult Scler.* 2013 October ; 19(11): . doi:10.1177/1352458513498124.

## EVOLUTION OF TUMEFACTIVE LESIONS IN MULTIPLE SCLEROSIS: A 12-YEAR STUDY WITH SERIAL IMAGING IN A SINGLE PATIENT

Vasiliki N. Ikonomidou<sup>1,2</sup>, Nancy D. Richert<sup>2</sup>, Alexander Vortmeyer<sup>3</sup>, Fernanda Tovar-Moll<sup>2</sup>, Bibiana Bielekova<sup>2</sup>, Natalie E. Cook<sup>2</sup>, Jeff H. Duyn<sup>4</sup>, and Francesca Bagnato<sup>2,5</sup>

<sup>1</sup>Department of Bioengineering, Volgenau School of Engineering, George Mason University, Fairfax, VA, USA

<sup>2</sup>Neuroimmunology Branch, National Institute of Neurological Disorders and Stroke (NINDS), National Institutes of Health (NIH), Bethesda, MD, USA.

<sup>3</sup>Neurosurgery Branch, NINDS, NIH, Bethesda, MD.

<sup>4</sup>Advanced MRI section, LFMI, NINDS, NIH, Bethesda, MD, USA.

<sup>5</sup>Department of Neurology, University of Maryland, Baltimore, MD, USA.

### Abstract

**Objective**—We describe the acute presentation and the long-term evolution of recurrent tumefactive lesions (TLs) in a patient with relapsing-remitting multiple sclerosis.

**Background**—Five TLs occurred at three separate timepoints over 12 years and these were followed by 73 serial magnetic resonance images.

**Methods**—TL evolution was described by means of magnetization transfer (MT) imaging and cerebrospinal fluid tissue specific imaging (TSI) over the period of the follow-up.

**Results**—During the study period, the patient had three clinical relapses with only minimal disability progression. MT imaging demonstrated that only the peripheral portion of each TL reverted to pre-lesional MT ratios within six months post-enhancement.

**Conclusions**—Recurring TLs may present a similar pattern of recovery that may be associated with a long-term favorable clinical outcome.

### Keywords

Multiple sclerosis; tumefactive lesion; magnetic resonance imaging; recovery; magnetization transfer imaging; tissue specific imaging

### CASE HISTORY

Our case study aims at (1) delineating the acute appearance and recovery pattern of five tumefactive lesions (TLs), analyzed over 12 years using 73 magnetic resonance imaging (MRI) exams, and (2) describing the long-term clinical outcome of a relapsing-remitting multiple sclerosis (RRMS) patient presenting multiple TLs (Fig.1A-D). A 36-year old woman presented to the NIH with bilateral leg numbness in September 1997. A year prior

she had a spontaneously resolving optic neuritis. Diagnosis of clinically definite MS was made and she enrolled in a clinical trial investigating the efficacy of the altered peptide ligand, CGP77116 (APL)<sup>1</sup>. After five months of therapy, she developed superior homonymous quadrantanopsia and TL1 (Fig. 1A). TL1 had started as a small enhancing lesion three months prior to evolving into a nodular TL with moderate edema, compression of the posterior horn of the right lateral ventricle and minimal midline shift. TL1 enhanced for seven months total. APL was discontinued. The patient responded well to a 10-day course (1 gram/day) of intravenous methylprednisolone (IVMP). Therapy with 6,000,000 i.u. Interferon beta-1a (IFN $\beta$ -1a) once weekly was initiated intramuscularly. In May-2000 (15 months later) she presented difficulty in retrieving words and weakness in the left extremities. Brain imaging showed a nodular TL2 and a partial-ring<sup>2</sup> TL3 (Fig. 1B) in the right anterior and left posterior fronto-parietal regions, respectively. These TLs had minimal mass effect towards the lateral ventricles but no midline shift. Both TLs enhanced for a total of four months. A stereotactic biopsy with immunohistochemistry was performed on TL3. Biopsy was performed because of concerns that this highly recurrent pattern could represent a malignancy. TL3 was chosen because of its surgical accessibility. A dense inflammatory infiltrate of lymphocytes with myelin loss and reduced axons was seen (Fig. 1E-L).

The patient tested negative for neutralizing antibodies against IFN $\beta$ . She was proposed adding Azathioprine to IFN $\beta$ -1a but she preferred continuing IFN $\beta$ -1a alone. In October-2002, because of persisting contrast-enhancing lesion activity (Fig. 1D) Daclizumab (120 milligrams IV once monthly) was added and continued alone from June-2003 until December-2003. Three months after Daclizumab discontinuation she developed right optic neuritis which remitted completely on a 5-day course of IVMP. Due to this clinical exacerbation, in June-2004 therapy with daily subcutaneous Glatimerar Acetate was initiated. Nine months later TL4 and TL5 (Fig. 1C) were incidentally seen during a 3T research imaging study. TL4 was located in the left frontal lobe adjacent to the lateral ventricle with no mass effect. TL5 appeared in the right medial parietal lobe with minimal mass effect on the posterior horn of the lateral ventricle. Both TLs had nodular shape and none exerted midline shift. Although the patient did not report new symptoms, due to the presence of the two TLs she underwent a 10-day course of IVMP. Glatimerar Acetate was discontinued. IFN $\beta$ -1a at the dose of 44 mcg subcutaneously three times per week was started in association with monthly IVMP for six months. The patient remained free from clinical relapses until May-2010 (54 months, study-year 12) when disability at the Expanded Disability Status Scale<sup>3</sup> was rated at 2.5. She has not returned to the NIH since.

### TLs evolution

Image acquisition and processing details are reported in the *online* material. A voxel-based analysis of TL1 (representative example) showed a mild decline in magnetization transfer ratio (MTR) in normal-appearing white matter several months before the enhancement (Fig. 2A). During the TL acute phase, MTR showed a further sharp decrease. Significant recovery was seen within six months and was stable throughout the follow-up (Fig. 2B) but only voxels enhancing at the lesion periphery (Fig. 2C-E) returned to baseline MTR values. Two years after the acute enhancement of each TL, the percentage of recovering voxels was 61% (TL1), 51% (TL2) and 38% (TL3, biased by scar tissue post-biopsy), 71% (TL4) and 62% (TL5). Only 27.5% (TL4) and 25.8% (TL5) of the central enhancing voxels were visible in cerebrospinal fluid tissue specific imaging (CSF-TSI)<sup>4,5</sup> in the acute phase. Two years later, only 4.6% (TL4) and 5.9% (TL5) of these voxels remained hyperintense in CSF-TSI.

## DISCUSSION

The TL appearance and recovery patterns seen in our patient resemble the ones of type-I and II active lesions described by previous authors<sup>6</sup>. These types of lesions generally start with profound blood brain barrier damage, massive edema, demyelination and pronounced axonal destruction. When the lesions mature edema resolves; there is profound remyelination throughout the lesions, but because of axonal injury in the center of the lesion, repair is incomplete. In our case, sharp decreases in MTR and hyperintense signal in CSF-TSI were seen during the TL enhancement and, as confirmed by histopathology, indicated severe myelin damage, inflammatory infiltrates and axon decomposition. Over time, only MTRs of peripheral voxels reverted to pre-lesion values, consistent with the notion of an incomplete recovery and axonal injury predominantly in the central core of the TL.

In our patient, the first TL occurred during the administration of the experimental drug APL<sup>1</sup>. The relation between TLs first appearance and APL is a unique aspect of our case compared to previous literature. It remains unknown, however, if the APL was the actual cause of TL multiple occurrences. Three elements do not appear to support this hypothesis. First is the fact that none of the other patients enrolled in the experimental clinical trial developed TLs<sup>1</sup>. Second the fact that three patients in the APL trial that had MS exacerbations. Only in the other two patients who experienced clinical exacerbations, we were able to mechanistically link these exacerbations to the increase in MBP (83-99)-specific T cells, cross-reactivity to the APL<sup>1</sup>. Third is the notion that as seen in our patient, TLs tend to present predominately in female RRMS patients and during the third decade of life<sup>7,8</sup>. TL reoccurrence is rarely seen, however. In a large cohort of 54 MS patients with TLs followed for a median time of 38 months, TLs re-occurred twice in about 20% of the patients and three times in less than 2%<sup>9</sup>. The relatively high reoccurrence rate seen in our patient may be partially explained by the longer follow-up period.

In conclusion we confirm that TLs may reoccur in MS. We demonstrate that when reoccurring TLs may present with a homogenous imaging pattern of recovery over time and may be associated with an overall favorable clinical prognosis.

## Acknowledgments

This research was supported by the Intramural Research Program of the NINDS-NIH. We are grateful to the patient whose findings are herein presented for the time and cooperation required for participating in the study. We thank Drs Joseph Frank and Peter van Geldern for help with some of the data acquisition. The authors are grateful to Prof. Hans Lassmann from the Medical University in Vienna for his helpful insights.

## APPENDIX

### Scanning protocol

#### 1.5T MRI

Seventy-one magnetic resonance images (MRIs) were obtained at 1.5 Tesla (1.5T) (General Electric Medical Systems, Milwaukee, WI, USA) using a standard quadrature head coil. Imaging sequences included: (1) dual echo proton density and fast spin echo (FSE) T<sub>2</sub>-weighted (T<sub>2</sub>-w) images with echo time (TE) 20/100 ms, repetition time (TR) 2000 ms, and two excitations; (2) T<sub>1</sub>-w spin echo (SE) images with TE 16 ms, TR 600 ms, two excitations, acquired both before and after contrast injection (0.1 mmol/kg) with Gd-DTPA (Magnevist, Berlex Laboratories, Wayne, NJ, USA); (3) an additional T<sub>1</sub>-w SE image obtained pre-contrast injection with (M<sub>s</sub>) a saturation pulse (16 msec, 1.2 kHz below water frequency, 95° flip angle), used together with the T<sub>1</sub>-w SE image obtained pre-contrast without the saturation pulse (M<sub>0</sub>) in order to calculate magnetization transfer ratio (MTR)

maps.<sup>1</sup> All images were obtained using 3 mm thick slices without gap with 24 cm field of view (FOV) and a matrix size of 128×256. Total scan time was about 45 minutes.

### 3T MRI

Two MRI scans were acquired using a 3T magnet (General Electric Medical Systems, Milwaukee, WI, USA) equipped with the product 8-channel receive-only head array. Imaging sequences included: (1) FSE T<sub>2</sub>-w with TE 120 ms and TR 5/100 ms and (2) pre- and post- (Gd-DTPA) contrast SE T<sub>1</sub>-w with TE 11 ms and TR 700 ms. All images were obtained using contiguous 2.4 mm slices with 24-cm FOV and matrix 256×256. At 3T, tissue specific imaging (TSI)<sup>2</sup> was also acquired. TSI is an MRI technique that offers simultaneous acquisition of three images, corresponding to white matter (WM), gray matter (GM) and cerebrospinal fluid (CSF). TSI was implemented as previously described.<sup>2</sup> Briefly, during each 6-second TR, three echo planar images were acquired at times of 0 ms, 3,675 ms and 5,821 ms, with FAs 83°, 17° and 62°. Two adiabatic inversion pulses were employed at 3,195 ms and 5,383 ms. SENSE rate 2 acceleration was used to achieve whole brain coverage with matrix size 144×112×110 with 1.5 mm<sup>3</sup> isotropic resolution in 11 minutes. TE was set to 35 ms. Navigator echo correction was used to minimize phase errors between subsequent excitations. The resulting raw images were combined assuming average T<sub>1</sub> values of 800 ms, 1,550 ms and 4,000 ms for WM, GM and CSF respectively. CSF-TSI is one of the three images produced by TSI, which selectively visualizes CSF in healthy brains and lesions with higher amount of fluid accumulation in MS patients.<sup>3,4</sup> The other two, WM-TSI and GM-TSI, visualize white matter and gray matter respectively. The three images are generated automatically but for the goals of the present study we focused on the CSF-TSI only.

### Image post-processing

For the first three tumefactive lesions (TLs) multiple MTR images were acquired at 1.5T. For TL4 and TL5 we have a similar longitudinal MRI data set except that MTI was not available during the acute phase and 3T CSF-TSI was used for the description of imaging details of the acute phase of the TLs.

### Identification and measurement of contrast enhancing lesions (CELs)

CELs and TLs were identified on hard copy films of post-contrast images and subsequently marked on electronic form for creation of a mask image and volumetric measurements using the Medical Image Processing, Analysis and Visualization (MIPAV) package (<http://mipav.cit.nih.gov>). A total of 73 MRIs were inspected for the presence of CELs and TLs.

Regions of interest (ROIs) were marked on the post-contrast T<sub>1</sub>-w image of the acute phase, covering the enhancing portion for nodular lesions and the sum of the enhancing and central portion for the ring lesions.<sup>5</sup> In the case of TL3, the ROI was manually edited to exclude the biopsy scar. ROIs were automatically edited to exclude areas that in previous examinations displayed MTR values less than 0.32<sup>6</sup>, indicative of the expansion of the ROI into gray matter due to mass effect.

### MTI analysis

For the MTR calculation, the T<sub>1</sub>-w M<sub>S</sub> and M<sub>0</sub> images were registered to each other using an affine registration algorithm with 6 degrees of freedom as implemented in MINC tools.<sup>7</sup>

Subsequently, MTR maps were calculated based on the formula  $MTR = \frac{M_0 - M_s}{M_0}$ . To account for scanner drift, MTR values were normalized based on the MTR of an ROI that remained NAWM throughout the study.

## MTR analysis

For each TL, MTR maps from all exams were registered to the post-contrast T<sub>1</sub>-w image corresponding to its acute phase, using an affine transformation with 6 degrees of freedom. ROIs of the TL enhancement were overlaid on the registered MTR maps.

Within each TL ROI and on a voxel by voxel basis, MTR values computed at each time point were compared with a baseline-MTR. Baseline MTRs were calculated based on the average MTR map of the first four monthly MRIs (August 1998 – October 1998); for each TL, the average and the standard deviation of the MTR were calculated in the TL ROI and used as reference for establishing which voxels recovered. The first four monthly MRIs appeared to precede the occurrence of TL1 by three months and by 19 months the occurrence of TL2 and TL3. Care was taken to ensure that during baseline, these regions corresponded to WM appearing as normal on T<sub>2</sub>-w image. Voxels were considered as “recovered” if their MTR value was greater than the mean minus two standard deviations of the baseline. For each time-point in the follow-up, we calculated (a) on a voxel-by-voxel basis, the percentage of voxels returning to MTR values within two standard deviations of the baseline, and (b) the average MTRs in the central (non-recovered) and the periphery (recovered) regions of the TLs. The latter was calculated using ROI analysis; we defined the recovered and non-recovered voxels based on the MTR images.

For 1.5T, 18 MRIs preceding and 49 MRIs following the lesion were available for the TL developed in January 1999 (TL1); 32 MRIs preceding and 35 MRIs following the lesions were available for the TLs developed in May 2000 (TL2 and TL3); 61 MRIs preceding and seven MRIs following the lesions were available for the TLs developed in May 2005 (TL4 and TL5). MTR data from three additional 1.5T acquisitions were excluded due to image artifacts. Additionally, the MTIs were available only until October-2007, making 44 MRIs following TL-1 (developed in January 1999), 31 MRIs TL-2 and TL-3 (developed in May 2000) and three MRIs following the TL-4 and TL-5 (developed in May 2005).

## REFERENCES

1. Bielekova B, Goodwin B, Richert N, et al. Encephalitogenic Potential of the Myelin Basic Protein Peptide (amino Acids 83-99) in Multiple Sclerosis: Results of a Phase II Clinical Trial with an Altered Peptide Ligand. *Nat Med.* 2000; 6:1167–1175. [PubMed: 11017150]
2. Davis M, Auh S, Riva M, et al. Ring and nodular multiple sclerosis lesions: a retrospective natural history study. *Neurology.* 2010; 74:851–856. [PubMed: 20211910]
3. Kurtzke JF. Rating Neurologic Impairment in Multiple Sclerosis: An Expanded Disability Status Scale (EDSS). *Neurology.* 1983; 33:1444–1452. [PubMed: 6685237]
4. Ikonomidou VN, van Gelderen P, de Zwart JA, et al. Optimizing brain tissue contrast with EPI: a simulated annealing approach. *Magn Reson Med.* 2005; 54:373–385. [PubMed: 16032676]
5. Riva M, Ikonomidou VN, Ostuni JJ, et al. Tissue-specific Imaging Is a Robust Methodology to Differentiate in Vivo T1 Black Holes with Advanced Multiple Sclerosis-induced Damage. *AJNR Am J Neuroradiol.* 2009; 30:1394–1401. [PubMed: 19406765]
6. Lucchinetti CF, Bruck W, Parisi J, et al. Heterogeneity of multiple sclerosis lesions: implications for the pathogenesis of demyelination. *Ann Neurol.* 2000; 47:707–717. [PubMed: 10852536]
7. Lucchinetti CF, Gavrilova RH, Metz I, et al. Clinical and Radiographic Spectrum of Pathologically Confirmed Tumefactive Multiple Sclerosis. *Brain.* 2008; 131:1759–1775. [PubMed: 18535080]
8. Comi G. Multiple Sclerosis: Pseudotumoral Forms. *Neurol Sci.* 2004; 25(Suppl 4):S374–379. [PubMed: 15727238]
9. Altintas A, Petek B, Isik N, et al. Clinical and Radiological Characteristics of Tumefactive Demyelinating Lesions: Follow-up Study. *Mult Scler.* 2012; 18:1448–1453. [PubMed: 22419670]

## REFERENCES FOR ONLINE APPENDIX

1. Richert ND, Ostuni JL, Bash CN, et al. Interferon beta-1b and intravenous methylprednisolone promote lesion recovery in multiple sclerosis. *Mult Scler.* 2001; 7:49–59. [PubMed: 11321194]
2. Ikonomidou VN, van Gelderen P, de Zwart JA, et al. Optimizing Brain Tissue Contrast with EPI: a Simulated Annealing Approach. *Magn Reson Med.* 2005; 54:373–385. [PubMed: 16032676]
3. Riva M, Ikonomidou VN, Ostuni JJ, et al. Tissue-specific Imaging Is a Robust Methodology to Differentiate in Vivo T1 Black Holes with Advanced Multiple Sclerosis-induced Damage. *AJNR Am J Neuroradiol.* 2009; 30:1394–1401. [PubMed: 19406765]
4. Bagnato F, Ikonomidou VN, van Gelderen P, et al. Lesions by Tissue Specific Imaging Characterize Multiple Sclerosis Patients with More Advanced Disease. *Mult Scler.* 2011; 17:1424–1431. [PubMed: 21803873]
5. Davis M, Auh S, Riva M, et al. Ring and nodular multiple sclerosis lesions: a retrospective natural history study. *Neurology.* 2010; 74:851–856. [PubMed: 20211910]
6. Ge Y, Grossman RI, Babb JS, et al. Age-related Total Gray Matter and White Matter Changes in Normal Adult Brain. Part II: Quantitative Magnetization Transfer Ratio Histogram Analysis. *American Journal of Neuroradiology.* 2002; 23:1334–1341. [PubMed: 12223374]
7. Collins DL, Neelin P, Peters TM, Evans AC. Automatic 3D intersubject registration of MR volumetric data in standardized Talairach space. *J Comput Assist Tomogr.* 1994; 18:192–205. [PubMed: 8126267]

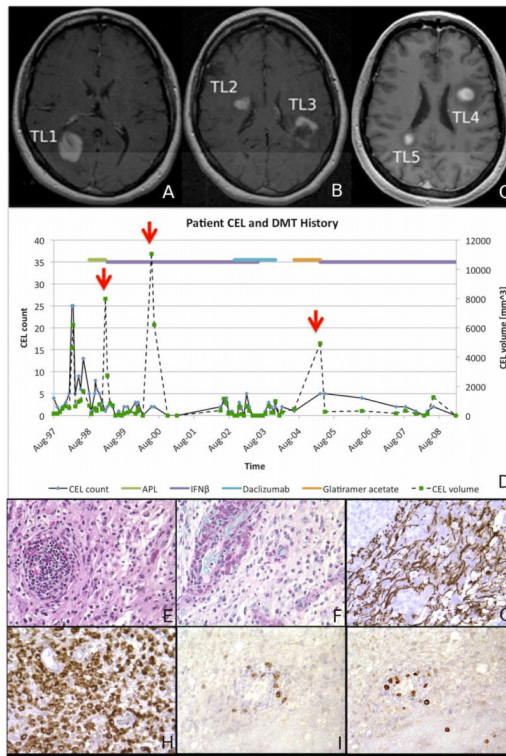


#### FIGURE 1. ACUTE APPEARANCE OF TL

Post-contrast T<sub>1</sub>-weighted images obtained in January 1999 (**Figure 1A**), May 2000 (**Figure 1B**) and March 2005 (**Figure 1C**) showing the presence of the five TLs at the time of their first appearance. MRIs in figures 1A and 1B were acquired at 1.5 Tesla. MRI in figure 1C was acquired at 3.0 T. **Figure 1D** summarizes patient history, showing the number (black solid line) and volume (black dashed line) of contrast-enhancing lesions counted and measured on each MRI. The red arrows indicate times when the TLs were seen. Horizontal lines on the top indicate the various treatments the patient was exposed to. Over the 12-year follow-up, non-TL active lesions were visible in 56 (77%) of 73 imaging studies. The panel in Figure 1E-J depicts the histopathological correlates of TLs. Hematoxylin-Eosin stain shows a focal perivascular inflammatory infiltrate composed of lymphocytes, macrophages, and reactive astrocytes (**Figure 1E**). PAS stain reveals PAS-positive granules in numerous macrophages (perivascular and intraparenchymal) (**Figure 1F**). Immunohistochemistry for neurofilament protein shows preserved, though rarefied axonal structures (**Figure 1G**). Immunohistochemistry for CD68 antigen reveals an abundance of microglial/macrophagocytic cells, which appear to represent the predominant cytologic component in this inflammatory process (**Figure 1H**). Immunohistochemistry for CD20 (B cells) (**Figure 1I**) and CD8 (T cells) (**Figure 1J**) shows positive cells predominantly within perivascular spaces.

In the figure: DMT=disease modifying therapy; IFN $\beta$ =interferon beta, CEL=contrast enhancing lesion.

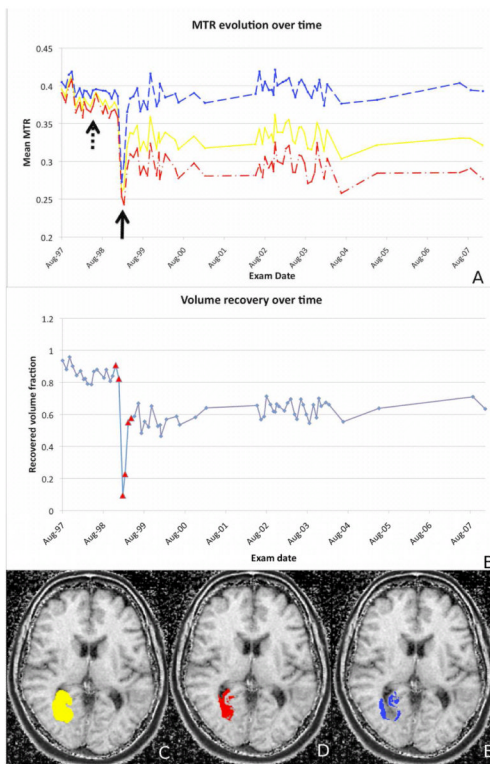


**FIGURE 2. TL EVOLUTION OVER TIME**

Mean MTR changes (**Figure 2A**) over the follow-up period for the whole TL1 (solid line), the peripheral region (dashed line) and the central core (dash-dot line). A sharp decrease in MTR affected almost the entire enhancing area in the acute phase (black solid arrow). Smaller MTR declines preceded the acute phase by 12 months (black dotted-line arrow). Signs of recovery were seen as early as six months after TL first appearance. We depict the percentage of TL1 voxels returning to baseline MTR (**Figure 2B**) over the period of the follow-up. Enlarged triangular dots denote MRIs showing some enhancement in the region of the TL. Maps of the areas of lesion recovery is represented in figure 2C-E, showing in **Figure 2C** the entire lesion, in **Figure 2D** voxels that did not recover and in **Figure 2E** voxels that recovered over time.